

Technical Notes

TECHNICAL NOTES are short manuscripts describing new developments or important results of a preliminary nature. These Notes cannot exceed 6 manuscript pages and 3 figures; a page of text may be substituted for a figure and vice versa. After informal review by the editors, they may be published within a few months of the date of receipt. Style requirements are the same as for regular contributions (see inside back cover).

Analysis of Crystalline Phase Aluminum Oxide Particles from Solid Propellant Exhausts

K. M. Dill*

Sverdrup Technology, Inc.

Arnold Air Force Station, Tennessee 37389

R. A. Reed†

Sverdrup Technology, Inc.

Arnold Air Force Base, Tennessee

V. S. Calia‡

Grumman Aerospace Corporation, Bethpage, New York
and

R. J. Schulz‡

University of Tennessee Space Institute
Tullahoma, Tennessee

Introduction

ALUMINUM oxide particles in the exhaust of solid propellant rocket motors are found to occur in at least two different major crystalline phases, alpha and gamma. This is believed, on rather general grounds, to be related to the temperature-time history of the particles, but no quantitative explanation has yet been afforded. The possibility of retrieving nozzle flowfield information from the measured alpha/gamma ratio provides one motivation for the present work. The abundance of the gamma phase is also of interest to atmospheric scientists because it is an efficient catalyst for many surface reactions. Finally, knowledge of the crystal phase of Al_2O_3 in rocket exhaust is needed for analysis of plume thermal emission. As a first step in meeting these needs, a new analytical technique for determining the alpha/gamma ratio has been developed based upon far-infrared absorption spectroscopy. The technique appears to be superior to x-ray diffraction and shows promise for future in-situ application. The technique was applied to several rocket particle samples collected during full-scale motor firings conducted in an Arnold Engineering Development Center (AEDC) altitude chamber simulation facility. The preponderance of each sample, from 64 to 93% by mass, was found to be composed of a fine grained gamma phase which was not readily detected by standard x-ray diffraction methods.

Rocket Particle Measurement

Both alpha and gamma phase Al_2O_3 have been identified in particles collected from solid propellant rocket exhaust plumes.^{1,2} The thermophysical properties of these two phases are given in Table 1. The general indication is that the smaller

particles tend to be gamma phase, and the larger ones tend to be alpha phase. This is consistent with the observation that gamma phase is produced by rapid temperature quenching of the liquid.^{3,4}

The aluminum oxide particles of this investigation were collected in the near-field exhaust plumes of three different rocket motors during static firings at simulated altitude conditions of approximately 100,000 ft. The samples were obtained from the PAM D-II (Morton Thiokol Corp.), IUS (United Technologies Chemical Systems Div.), and Peacekeeper Stage II (Aerojet Strategic Propulsion Co.) rocket motors, which are herein denoted motor numbers 1, 2, and 3, respectively. A tungsten-tipped, water-cooled, quench-type sampling probe was inserted into the hot exhaust flow approximately 8 ft downstream of the nozzle exits allowing particles to be collected before they impinged upon the test cell walls. The water quenching design allowed for the transport of the particles from the probe entry tip to collection bottles. The particles then underwent numerous washings and filterings to remove acids (principally HCl). About 30 g of material were collected from each firing. Most samples were collected at the edge of the plume, but a few were taken from the centerline. There were no significant differences in either size or composition between centerline and edge samples. A typical scanning electron microscope (SEM) photograph of the samples is shown in Fig. 1. As can be seen, many of the collected particles are really an agglomeration of several smaller particles. The sizes of the agglomerated particles sampled by the SEM are summarized in Table 2. Most of the particles are between 0.1 and 1 μ . Size analysis by Coulter counter⁵ was in substantial agreement with Table 2. A full description of the rocket test facility and particle sampling work is given in Ref. 1.

Although the usual procedure for determining crystal structure is x-ray powder diffraction, several methods actually exist, as shown in Table 3. An x-ray diffraction analysis of the samples at the Sandia National Laboratory⁶ and at the Grumman Aerospace Corporation both indicate that the rocket particles were predominately in the alpha phase, with small amounts of gamma in some samples, and no discernible gamma at all in other samples. Since it is sometimes difficult to obtain quantitative x-ray diffraction data on fine powders, an alternative method was sought to check this result. On the basis of the differences in crystal structure (cubic vs hexagonal), it was decided that long-wavelength, infrared-absorption spectral analysis might provide a quantitative method to deter-

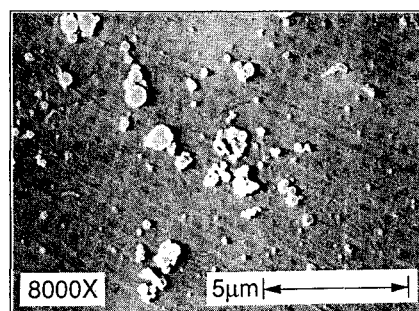


Fig. 1 Typical scanning electron microscope photo of particulate sample.

Received March 21, 1988; revision received July 12, 1989. This paper is declared a work of the U.S. Government and is not subject to copyright protection in the United States.

*Propulsion Engineer, AEDC Group; currently, MSFC Group, Huntsville, AL 35806.

†Senior Engineer, Arnold Engineering Development Center Group.

‡Associate Director, Fluid Mechanics Branch.

§Associate Professor.

mine the relative amounts of alpha and gamma Al_2O_3 present in the samples. This was confirmed using commercial dual-beam infrared spectrometer transmission measurements through particles suspended in a transparent KBr pellet. The transmission spectra of a 0.3–0.6 μ diam alpha sample (Sumitomo, Inc., AKP-HP, 99.995% purity) is shown in Fig. 2 and that of an under 0.1 μ diam gamma sample (Sumitomo, Inc., AKPG, also 99.995% purity) is shown in Fig. 3. Whereas the alpha phase shows two distinct absorption features near 450 and 600 cm^{-1} , the gamma phase shows only a single broad absorption from roughly 500–900 cm^{-1} . A calibration curve for determining the alpha/gamma ratio in mixtures was made using a series of reference samples with alpha mass fractions of 0, 10.4, 56, 89.4, and 100%. At present, the calibration curve is based upon the ratio R of absorbencies (i.e., negative log of transmission) at 450 cm^{-1} vs 570 cm^{-1} (alpha). This ratio increases linearly with gamma mass fraction ranging from approximately unity for a pure alpha sample to a value near two for a pure gamma sample. The estimated accuracy of the procedure is 5–10%, which is comparable to the accuracy of a careful x-ray analysis using internal standards such as KNO_3 or zirconia.

Table 1 Thermophysical properties of alpha and gamma Al_2O_3

Property	Alpha	Gamma
Crystal structure	Hexagonal	Cubic
Density (g/cm^3 at 298 K)	3.98	3.5
Heat of formation (Kcal/mole at 298.15 K)	–400.4	–396
Heat capacity, C (cal/g-mole K at 298.15 K)	18.889	19.773
Melting point, K	2324	—

Table 2 Size distribution of alumina samples measured by SEM

Size range, μ	Percentage of particles ^a		
	Motor no. 1	Motor no. 2	Motor no. 3
0.1–0.2	12.1	30.8	21.0
0.2–0.3	15.0	23.5	20.4
0.3–0.4	19.7	19.0	13.7
0.4–0.5	10.8	10.7	14.2
0.5–0.6	10.7	5.7	7.7
0.6–0.7	6.7	2.5	5.1
0.7–0.8	4.5	1.6	4.3
0.8–0.9	3.9	2.3	3.0
0.9–1.0	2.9	0.6	2.9
>1.0	13.7	3.3	7.7

^aThe SEM was preset to measure particles in the 0.1–2.5 μ range (lower limit of the machine).

The infrared transmission spectra for the rocket particles were all fairly similar. A representative spectrum is shown in Fig. 4. Note that the characteristic alpha phase reststrahl band near 570 cm^{-1} (17 μ) is absent, clearly indicating that very little of the rocket material is alpha phase. The quantitative analysis of these spectra are in Table 4, where the gamma phase is seen to constitute between 64–93% by mass of the total rocket sample. This was an unexpected result, as previous x-ray analysis of these same samples had indicated a preponderance of alpha phase, with little or no evidence of the gamma form. In addition, samples of the Space Shuttle solid rocket booster exhaust collected off the launch tower structure and analyzed

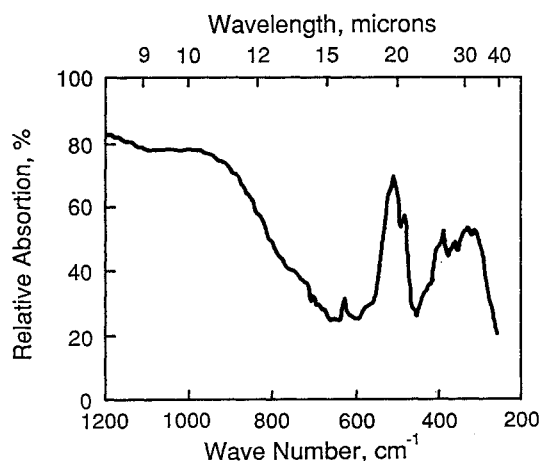


Fig. 2 Alpha aluminum oxide infrared absorption spectra.

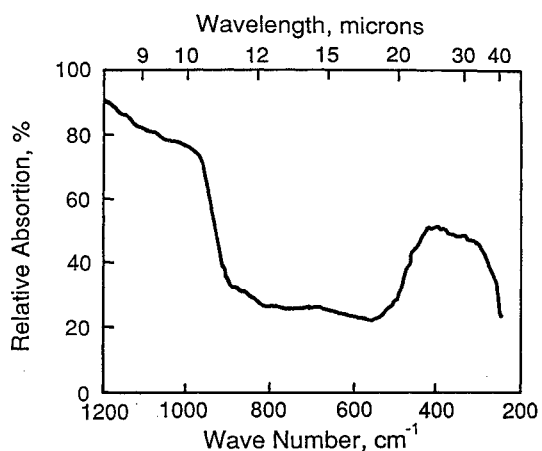


Fig. 3 Gamma aluminum oxide infrared absorption spectra.

Table 3 Methods for crystal-phase determination

Method	Pro	Con
X-ray diffraction	Semiquantitative for crystalline material	Inapplicable for amorphous or microcrystalline phases
Flotation/ sedimentation	Physically separates the two phases Conceptually simple to perform	Combustion particles may not have bulk density Particles could be porous
Acid solubility	Physically separates the two phases Conceptually simple	Does not discriminate between gamma- Al_2O_3 and other soluble species Experimentally difficult
Spectroscopy	Useful for microcrystalline and/or amorphous materials	Possible combustion effects (impurities in samples and unburned aluminum) Analysis of particles required $\leq 1 \mu$

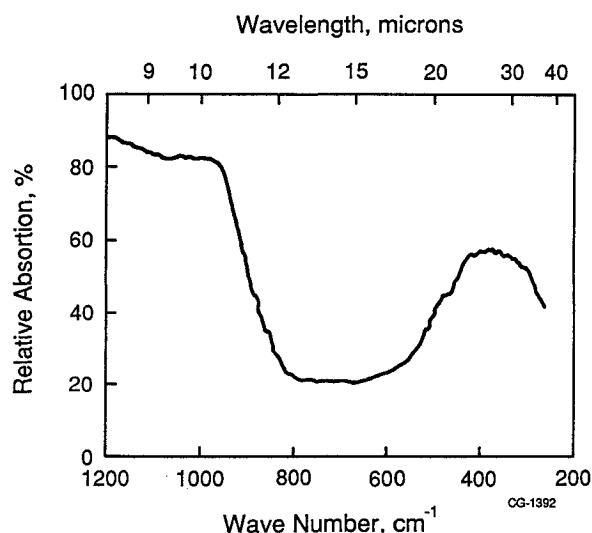


Fig. 4 Absorption spectra of representative sample of rocket exhaust Al_2O_3 particles.

Table 4 Mass fractions of alpha and gamma crystalline phases from different rocket motors^a

Rocket motor	Sample	% alpha	% gamma
PAM D-II	1	23	77
	2	24	76
	3	9	91
	4	7	93
Peacekeeper Stage II	1	32	68
	2	35	65
	3	36	64
IUS Solid Rocket Motor II	1	18	82
	2	14	86

^a Does not include metal impurities in the samples. They are a very small contribution to the total mass of the samples.

with the aqua regia method indicated alpha mass fractions in the range of 72–94% in six launches.²

Discussion

At present, the disagreement between the x-ray and infrared assays of the AEDC rocket particles is attributed to the intrinsically weak diffraction pattern of the gamma phase. The gamma x-ray lines are typically broad with only a few percent of the intensity of the alpha phase lines, which makes the lines easy to miss unless a careful background subtraction of the alpha peaks is first performed.⁷ This is attributed to particle crystalline domain size effects, which can vary from sample to sample. When the Sumitomo, Inc., gamma phase powder (size $< 0.1 \mu$) was subjected to x-ray diffraction analysis, for example, no gamma peaks were seen. The gamma phase peaks were evident, however, with a larger 0.5μ diam gamma sample from Cerac. Because of this sensitivity to crystalline domain size, it is recommended that the current practice of analyzing rocket samples with x-ray diffraction analysis should be revised to include an infrared analysis as well.

A final word regarding the kinetics of the gamma to alpha phase transition reaction is in order. Although gamma phase Al_2O_3 is stable at room temperature, it spontaneously converts to alpha phase at high temperatures. We are unaware of rate measurements at rocket exhaust temperatures, but extrapolation of the intermediate temperature rate data of Fig. 5, taken from Ref. 8, to 2330 K indicates a half life of roughly 350 μs for the gamma phase in a rocket exhaust. This suggests that the measured alpha to gamma ratio may depend upon the temperature-time history of the particles. This thermal history includes the nozzle flowfield, the external plume, and, possibly also the location and nature of the collection apparatus. Ideally, one would like to obtain an accurate representation of

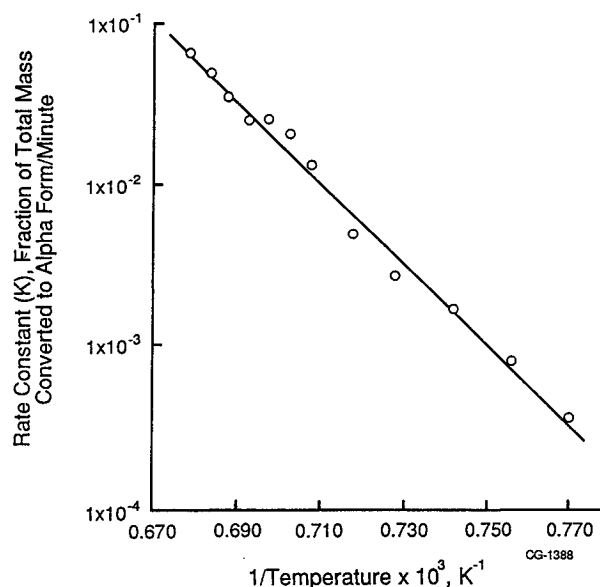


Fig. 5 Gamma to alpha transition rate constant as a function of temperature, Ref. 8.

the alpha to gamma ratio in the exhaust plume by providing an instantaneous temperature quench for the collection sample. The AEDC probe attempts to do this with an internal water spray, but the particles are also subjected to transient shock heating at the probe inlet. The possible effects of this transient heating and other probe effects upon the alpha/gamma ratio are unresolved at present, but the major conclusion of this investigation, the utility of the infrared method for phase analysis, remains valid. It should also be noted that particle temperature-time histories differ according to the source and method of particle collection, e.g., from an afterburning vs a nonafterburning plume, or from a rocket vs a quench bomb. Comparison of crystal phase data from different experiments may thus lead to needless confusion unless one accounts for the phase transition kinetics in a known thermal environment.

Acknowledgments

The research reported herein was performed by the Arnold Engineering Development Center, Air Force Systems Command. Work and analysis for this research were done by personnel of Sverdrup Technology, Inc./AEDC Group, operating contractor of the propulsion test facilities at AEDC. The authors wish to acknowledge Wheeler McGregor of Sverdrup Technology, Inc./AEDC Group, who initiated and continues to guide the particle sampling work. We also acknowledge Josephine Brewer of Analytical Research Associates, Inc., Columbus, OH; D. A. Nissen of Sandia National Laboratories, Livermore, CA; Al Tobin of Grumman Aerospace; and Randy Johnson of Schneider Services International, all of whom performed various assays of the particle samples.

References

- Girata, P. T., Jr., and McGregor, W. K., "Particle Sampling of Solid Rocket Motor (SRM) Exhausts in High Altitude Test Cells," AIAA Paper 83-0245, Jan. 1983.
- Cofer, W. R., III, Pellett, G. L., Sebacher, D., II, and Wakelyn, N. T., "Surface Chloride Salt Formation on Space Shuttle Exhaust Alumina," *Journal of Geophysical Research*, Vol. 89, No. D2, April 20, 1984, p. 2534.
- Plummer, M., "The Formation of Metastable Aluminas at High Temperature," *Journal of Applied Chemistry*, Vol. 8, 1958, pp. 35–44.
- Sokolowski, M., Sokolowska, A., Michalski, A., and Gokieli, B., "The In-Flame Reaction Method for Al_2O_3 Aerosol Formation," *Journal of Aerosol Science*, Vol. 8, 1977, pp. 219–230.
- Konopka, W. L., Reed, R. A., and Calia, V. S., "Measurements of Infrared Optical Properties of Al_2O_3 Rocket Particles," *Spacecraft Contamination: Sources and Prevention*, edited by J. A. Roux and

T. D. McKay, Vol. 91, Progress in Astronautics and Aeronautics AIAA, New York, 1984, pp. 180-196; also AIAA Paper 83-1568, 1983.

⁶Niven, D. A., private communication, Sandia National Laboratory, Livermore, CA.

⁷Benzel, J., private communication; Department of Ceramic Engineering, Georgia Institute of Technology, Atlanta, GA, 1989.

⁸Steiner, C. J.-P., Hasselman, D. P. H., and Spriggs, R. M., "Kinetics of the Gamma-to-Alpha Alumina Phase Transformation," *Journal of American Ceramics Society—Discussions and Notes*, Vol. 54, No. 8, Nov. 1971, p. 412.

Subatmospheric Burning Rates and Critical Diameters for AP/HTPB Propellant

Martin S. Miller* and Hughes E. Holmes†
U.S. Army Ballistic Research Laboratory
Aberdeen Proving Ground, Maryland 21005

Introduction

During the development of a base-bleed artillery round, it became desirable to measure the burning rate of the base-combustor propellant as a function of pressure at pressures low enough to simulate unchoked operation at altitudes up to 10 km. The results of these burning-rate measurements for two different propellants are described in this Note. Though burning rates were the objective of this study, the tendency of small-diameter strands to self-quench led us to give some attention to critical-diameter extinction phenomena.

The burning-rate measurements were conducted in a windowed strand burner modified for vacuum operation. The samples were burned cigarette fashion with a constant-flow-rate axial shroud of nitrogen gas helping to control smoke obscuration and inhibiting flamespread down the sides of the strand (no chemical inhibition of the sides was necessary). During a run the pressure was held constant to within 10%. Ignition of the sample was achieved by a resistively heated hot wire. Combustion of the sample was recorded using time-coded video and motion-analyzed with a video coordinate digitizer. The pressure associated with each burning rate is the average pressure during the measurement interval. Further experimental details may be found in Ref. 1.

Results

Two propellant formulations were investigated. The first, designated AP-1 here, consists of 73% (by weight) ammonium perchlorate (oxidizer), 14.95% hydroxy-terminated polybutadiene (binder), 5% oxamide (burn-rate modifier), 2% iron oxide (burning-rate modifier), 2% dioctyl azelate (plasticizer), 1.4% isophorone diisocyanate (curing agent), 1% zirconium carbide (ballistic modifier), 0.3% tapan (binding agent), 0.15% agerite white (anti-oxidant), 0.1% triphenyl bismuth (cure modifier), and 0.1% magnesium oxide (cure modifier). The second formulation, here termed AP-2, is the same except that the iron-oxide catalyst is omitted, being replaced with 1% AP and 1% oxamide. Strands of AP-2 were prepared employ-

ing cork borers of various diameters to core motor grains. The AP-1 tended to crack when this method was employed; therefore square strands were cut with a knife. The AP-1 strands were prepared and burned in a stable laboratory relative humidity of about 40%; however, during the AP-2 runs, the laboratory humidity increased to about 80-90%. To guard against possible inconsistencies arising from this variable, AP-2 strands were routinely placed in a desiccator after preparation and before combustion tests. Later tests showed that storage humidity did not influence the burning rate.

The AP-1 strands with 6.4-mm sides were burned with no difficulty at pressures down to 0.033 mPa and the measured burning rates are shown in Fig. 1 along with a least-squares fit to the usual power-law function. The remainder of this Note concerns only AP-2, which is the propellant of choice in the current application. AP-2 strands of 6.4 mm diam would not burn stably even at 0.1 mPa. This instability arose from the fact that this diameter is below the critical diameter for steady combustion. A plot of the burning rate as a function of strand diameter exhibits an abrupt fall-off near the critical diameter. For diameters at or slightly below the critical value, the strand typically ignites and burns about 1 cm before self-extinguishing. Over this distance the burning rate is about 85% of the value for "super-critical" (i.e., larger than critical) diameters. As the pressure decreases, the critical diameter in-

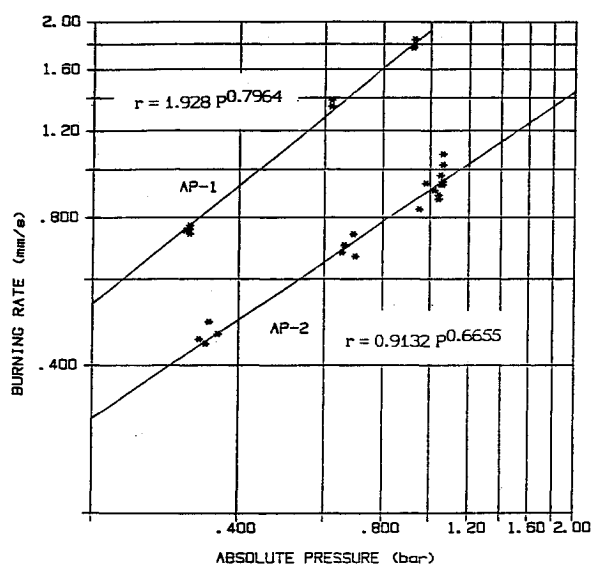


Fig. 1 Experimental burning rates and power-law fits.

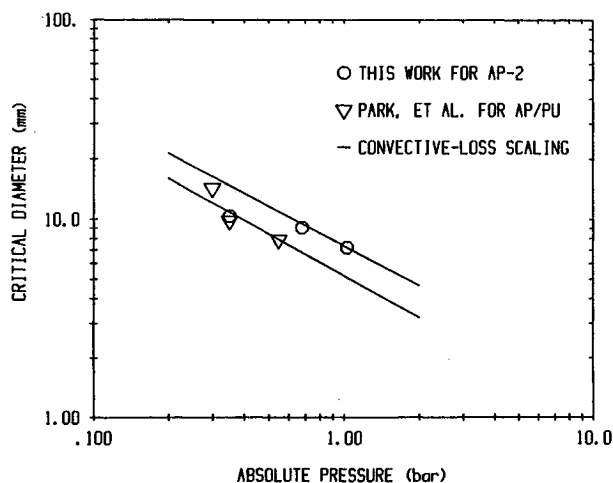


Fig. 2 Thresholds for self extinguishment.

Received Feb. 9, 1989; revision received May 10, 1989. This paper is a work of the U. S. Government and is not subject to copyright protection in the United States.

*Research Physicist, Ignition and Combustion Branch, Interior Ballistics Division.

†Physical Science Technician, Ignition and Combustion Branch, Interior Ballistics Division.